Chapter 4

FIRST PRINCIPLES STUDY OF IGNITION MECHANISM OF HYPERGOLIC BIPROPELLANT: N,N,N',N'-TETRAMETHYLETHYLENEDIAMINE (TMEDA), N,N,N',N'-TETRAMETHYLMETHYLENEDIAMINE (TMMDA) AND NITRIC ACID

Overview

Hypergolic bipropellants are fuel oxidizer pairs that ignite spontaneously upon mixing. Such propellants are useful for space propulsion because they can be fired any number of times by simply opening and closing the propellant valves until the propellants are exhausted. Common hyperbolic propellant combinations include nitrogen tetroxide (NTO)/monomethylhydrazine (MMH, MeHN-NH_2)[1, 2] and NTO/unsymmetrical dimethyl hydrazine (UDMH, Me_2N-NH_2)[3, 4]. However the carcinogenicity and toxicity of hydrazine derivatives makes it important to seek new low-toxicity hypergolic fuels[5]. Alkyl multiamines have been suggested as candidates to replace toxic hydrazine derivatives and experiments aimed at selecting the optimum saturated tertiary alkyl multiamines have been reported[6].

A common screen for the reactivity of bipropellants is the drop-test, which involves dropping fuel into the pool of oxidizer or vice versa. The *ignition delay*, defined as the time interval from the touch of two liquid surfaces to the appearance of a flame, is an indicator of reactivity. Among various alkylamines, N,N,N',N'-tetramethylethylenediamine (TMEDA) (Figure 4-1a) is considered as promising because of its short ignition delay[7] (14 ms) when reacting with white fuming nitric acid

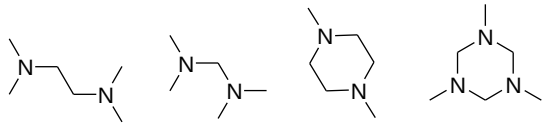

Figure 4-1. Structures of several alkyl amines (a) TMEDA (b) TMMDA (c) DMPipZ, (d) TMTZ

(WFNA), which consists of pure HNO_3 (no more than 2% water and less than 0.5% dissolved nitrogen dioxide or dinitrogen tetroxide). In contrast, N,N,N',N'-tetramethylmethylenediamine (TMMDA), a similar diamine linked by a single CH_2 group rather than two (Figure 4-1b) exhibits significantly longer ignition delay[8] (30ms) when reacting with white fuming nitric acid (WFNA). A similar dependence of ignition delay on the linker length is also observed in the drop-test of 1,4-dimethylpiperazine (DMPipZ, Figure 4-1c, 10ms ignition delay) with two linkers between the amines each with two CH_2 groups whereas 1,3,5-trimethylhexahydro-1,3,5-triazine (TMTZ, Figure 4-1d), with one CH_2 group is not hypergolic under the same experimental condition. The above results can be summarized as: *diamines linked by two CH_2 groups have much shorter ignition delay than those linked by a single CH_2.* Thus, even though ignition delay is a macroscopic measurement involving complex chemical and physical factors such as diffusion and thermal conduction, we find an atomistic level mechanism that explains the macroscopic phenomenon.

Based on the above observation and QM calculations (PBE flavor of DFT), McQuaid suggested a correlation between the ignition delay and the angle between orientations of the lone pair on nitrogen and the N-C/C-C bond[9]. Later, a QM mechanistic study (at G3MP2 level) of the early reaction between TMEDA and NO_2 was reported, in which an intermediate with C-C double bond was formed from the nitrite or nitro intermediate with both barriers higher than 23 kcal/mol[10]. The reaction mechanism of TMMDA and NO_2 has not previously been studied and no mechanism has yet explained why a CH_2-CH_2 linker between two amines leads to shorter ignition delay than for a single CH_2 group.

Wang et al.[7] proposed that the reaction between TMEDA and HNO_3 starts with an exothermic salt formation, in which the proton transfers from each of two HNO_3 molecules to each of the two nitrogen atoms on TMEDA to form the salt of alkyl diaminium and dinitrate anion (TMEDADN). The heat

released from the salt formation raises the local temperature at the interface between two liquids, leading to decomposition of HNO_3 into NO_2, O_2 and H_2O, followed by NO_2 reacting with TMEDA to form various free radicals and HONO, which is observed in the IR spectra in the gas product. The remaining free radicals would undergo further reaction, such as free radical recombination with NO_2 or breaking into smaller fragments, heating up the mixture and initiating more chain reactions. In this salt formation mechanism, two important factors have a major influence on the ignition delay:

(1) the exothermicity of the salt formation, and

(2) the rate of fuel molecules reacting with NO_2.

To investigate how the linker length affects these two factors, we considered the following questions:

1. How much energy is released when the nitrate salts of TMEDA and TMMDA are formed at the interface between two liquid surfaces?

2. What is the mechanism for TMEDA and TMMDA reacting with NO_2?

To approach the first question, we used the density functional theory (DFT) method with the B3LYP functional to calculate the energy release of TMEDA and TMMDA reacting with two HNO_3 molecules to form dinitrate salt using a dielectric cavity to model the solvent effect. The experimental measurement of ignition delay involves dropping the fuel into the pool of nitric acid. Therefore our calculations used solvent parameters taken from pure nitric acid to approximate the complex interface between the two liquid surfaces.

To answer the second question, we calculated all bond energies in TMEDA and TMMDA and compared with the bond energies for their alkane analogues to see how the presence of nitrogen atoms affects the bond energies. Furthermore, we carried out a mechanistic study on the system of TMEDA/NO_2 and TMMDA/NO_2 in gas phase at the same level of theory, calculating the potential energy surface and reaction pathway to determine how the reaction is initiated and how the connecting alkyl group can affect the reaction. We also studied the initiation reaction of TMEDADN/NO_2 and

the dinitrate salt of TMMDA (TMMDADN)/NO_2 in gas phase to determine how the salt formation changes the reactivity of such fuels.

Computational methods

All calculations were carried out with Jaguar 7.5 package, using the unrestricted hybrid functional UB3LYP to locate all stationary points and to calculate zero point energy and enthalpy using the 6-311G** basis set. All transition states (TS) were validated to have exactly one negative eigenvalue of the Hessian followed by the minimum energy path (MEP) scan to connect reactant and product. Thermodynamic data was evaluated at 298.15 K and 1 atm. Solvation effect was calculated using the Poisson-Boltzmann (PB) method as implemented in Jaguar, using the experimental dielectric constant (ε=50) and solvent radius ($R_{nitric\ acid}$=2.02Å) for pure nitric acid[11].

Results and discussion

The results are presented in the following manner. In Section 1 the heat of salt formation of both TMEDA and TMMDA are presented, with various bond energies in TMEDA, TMMDA and their alkane analogues in Section 2. Section 3 contains reaction mechanism for TMEDA reacting with NO_2 and Section 4 contains the mechanism of TMMDA reacting with NO_2. Section 5 compares how the molecular structure of TMEDA and TMMDA affects the reaction mechanisms. Seection 6 compares the initiation for NO_2 reacting with these two diamines and their dinitrate salts, TMEDADN and TMMDADN.

1. Exothermicity of the formation of dinitrate salt of TMEDA and TMMDA

Upon dropping TMEDA into a pool of HNO_3, condensed-phase TMEDA dinitrate is observed (using a high-speed camera) as a white cloud forming along the surface of the

contacting liquids[7]. In this reaction protons from HNO_3 are transferred to the N lone pairs on TMEDA and TMMDA as illustrated in (I) and (II).

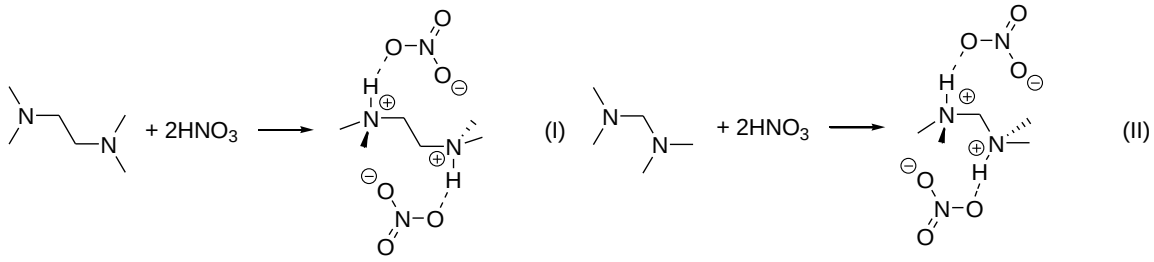

For TMEDADN, N-H distance is 1.058Å and O-H distance is 1.647Å while for TMMDADN, N-H distance is 1.062Å and O-H distance is 1.639Å. These short N-H bonds show that the protons are fully transferred to the N atoms to form a di-cation di-anion pair.

For reaction (I) to form TMEDADN, the total solution phase energy, which includes the QM electronic energy and the PB interaction of the molecule with the dielectric solvent cavity, is exothermic by 45.0 kcal/mol. For reaction (II), to form TMMDADN this reaction is downhill by 38.7 kcal/mol, which is 6.3 kcal/mol less exothermic than the formation of TMEDADN. The smaller energy release results from the shorter distance between two positive charged N atoms in TMMDADN (2.518Å) compared to 3.838Å in TMEDADN, leading to a larger electrostatic repulsion for the doubly protonation. The decreased exothermicity from forming TMMDADN should lead to a lower local temperature, contributing to the longer ignition delay of the reaction between TMMDA and HNO_3.

2. Bond energies in TMEDA, TMMDA and their alkane analogues

Although it is the barrier height that determines the reaction rate, one can often estimate the relative barriers from the changes in the bond energies, providing a hint about chemical reactivity.

The gas-phase bond energies in TMEDA, TMMDA and their alkane analogues, 2,5-dimethyl-hexane and 2,5-dimethyl-pentane are listed in Table 4-1. Particular points to note:

- The C^1-N^2 bonds in TMEDA and TMMDA are 7 to 10 kcal/mol weaker than the corresponding C-C bonds.
- The C-H bonds in TMEDA and TMMDA are 10 kcal/mol weaker than C-H bonds in the alkane.
- The C-C bond in TMEDA is significantly weaker by 18 kcal/mol than the corresponding C-C bond in its alkane analogue.

Thus the C^1-H bond energies in TMEDA and TMMDA are 86.3 and 86.4 kcal/mol, compared with the C-H bond energy in their alkane analogues, 96.6 and 96.2 kcal/mol. Similar reductions in bond energy are also found for C^3-H bonds. This is because after breaking the C-H bond, the free radical on C increases the strength of the C^3-N bond by ~10 kcal/mol due to the interaction with the lone pair electrons on N (a three-electron-two-center bond). This extra bonding between C and N stabilizes the final product and lowers the C-H bond energies. Such extra bonding can take place only if the free radical is adjacent to atoms having lone pairs.

By the same stabilization effect, the C^3-N^2 bond in TMMDA is weaker than the corresponding C^3-N^2 bond in TMEDA by 3 kcal/mol, and the drastically lower C^3-C^4 bond energy for TMEDA is due

Table 4-1. Bond energies in TMEDA, TMMDA, and their corresponding alkane analogues from B3LYP calculations

Bond Energies (kcal/mol)	TMEDA 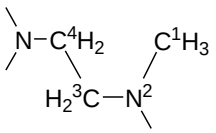	2,5-dimethyl-hexane 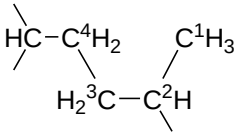	TMMDA 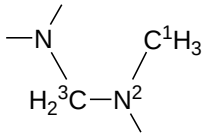	2,5-dimethyl-pentane 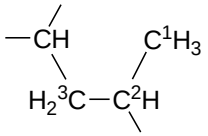
C^1-H	86.3	96.6	86.4	96.2
C^1-N^2/C^2	68.3	79.6	71.7	78.4
C^3-N^2/C^2	66.9	75.0	63.1	75.4
C^3-H	84.5	91.6	85.2	92.3
C^3-C^4	60.5	78.9	-	-

to the stabilization on both dissociation products. This makes this C-C bond the weakest bond in TMEDA, which is responsible for the fundamental difference in reactivity between TMEDA and TMMDA drastically lower than the one in its alkane analogue by 18 kcal/mol due to the stabilization on both dissociation products, rendering this C-C bond the weakest bond in TMEDA, which leads to the fundamental difference in reactivity between TMEDA and TMMDA.

3. Reaction mechanism of TMEDA+NO_2

The various stages of the reactions in gas phase between TMEDA and NO_2 are shown in Scheme 1, which can be categorized into 6 types:

1. H-abstraction by NO_2 to form HONO while leaving a free radical on C. (reactions to INT1, INT2, INT11 and INT12)
2. Trapping by NO_2 of the free radical formed by H-abstraction (leading to INT4, INT5, INT6 and INT8).
3. C-C double bond formation upon extraction of an H by NO_2, (leading to INT7) followed by reactions with NO_2 to form INT11 and INT12.
4. Rearrangement of INT4 and INT8 to break C-N bonds (leading to INT9, INT10, and INT13).
5. C-C bond breaking events: the C-C bond can be broken by simultaneous attack of two NO_2 on TMEDA (forming INT3), by the rearrangement of INT8 to form INT14 or INT15, or by the rearrangement of INT11 through a 4-member ring intermediate (INT16 or INT17) to form INT18.
6. Epoxide formation (INT19).

Figure 4-2 includes the enthalpy (no parentheses) and Gibbs free energy at 298.15K (in parentheses) of each species from the QM calculations, using the energies of separated TMEDA and NO_2 in the gas phase as the reference.

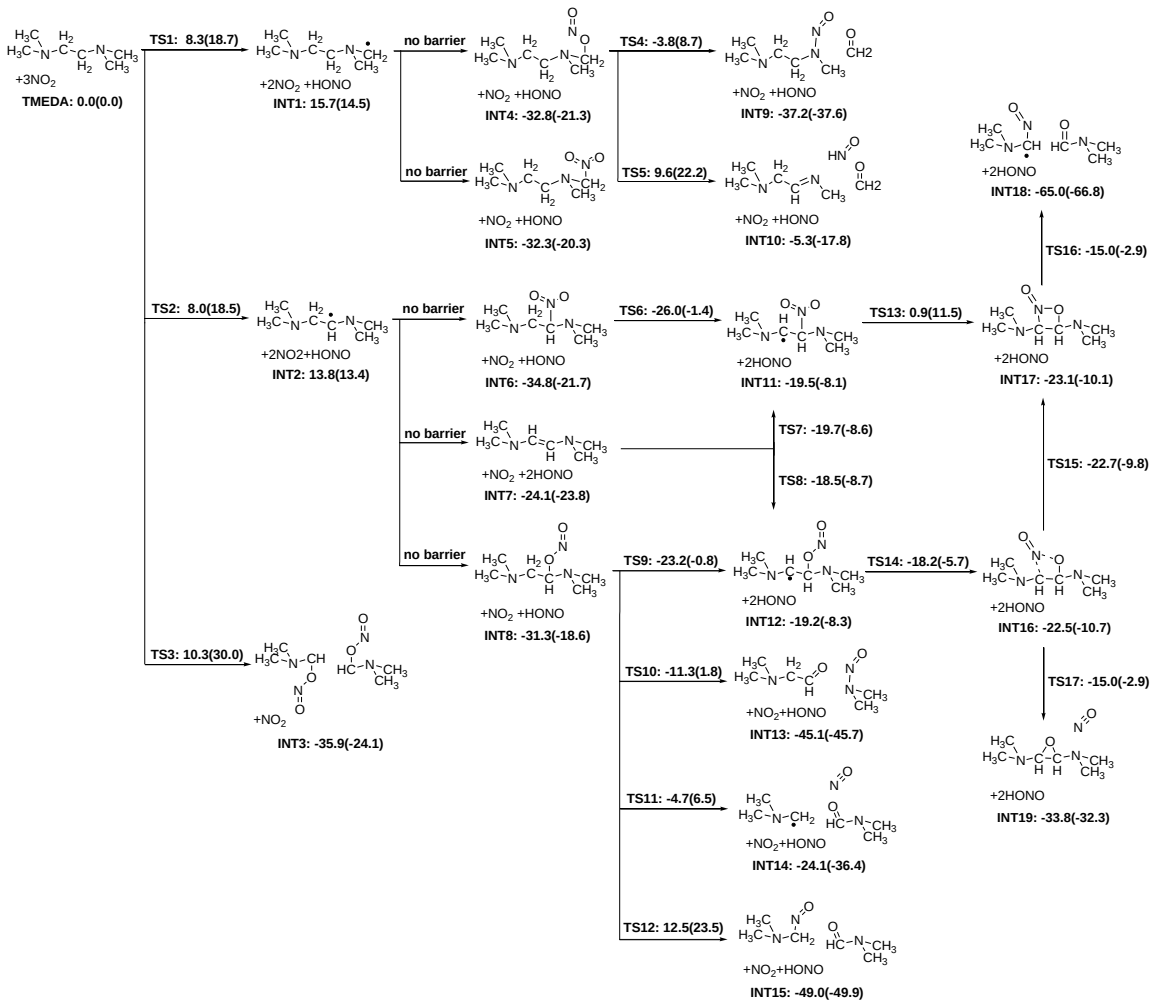

Figure 4-2. Reactions between TMEDA and NO_2. Enthalpy and Gibbs free energy at 298.15K (in parentheses) of each species are provided in kcal/mol.

3.1. Initiating stage

Based on MMH/NTO mechanism[12], where the HONO formation happens first, the reaction between TMEDA and NO_2 can be initiated with NO_2 abstracting the hydrogen on the terminal methyl group (TS1, Figure 4-3a) or the middle ethyl group (TS2, Figure 4-3b). There are three possible conformations for NO_2 abstracting H with different NO_2 orientation: 1. cis-HONO formation, 2. trans-HONO formation, 3. HNO_2 formation. We determined the barriers for various TS geometries and found that formation of *cis*-HONO is always the lowest, followed by the HNO_2 (higher by about 3

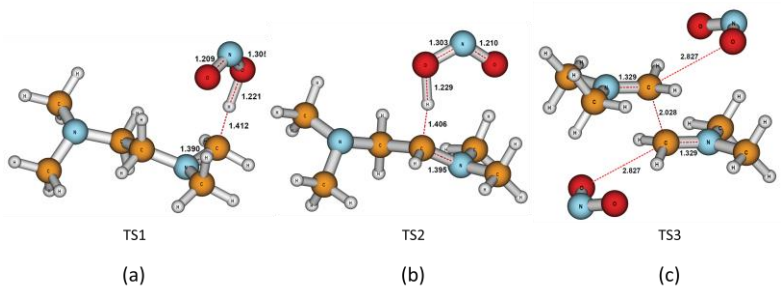

Figure 4-3. Structures of (a)TS1 (b)TS2 (c)TS3

kcal/mol) and then *trans*-HONO formation (higher by 7-8 kcal/mol), so only the TS for *cis*-HONO formation is reported here. The lower barrier for *cis*-HONO formation arises because of the improved interaction between the C-H bond and the A^1 radical orbital on NO_2 (in plane with the higher amplitude on the oxygens, same phase[13]). For *trans*-HONO formation, the TS has the distance of the H from the second O about 1Å longer than the one in *cis* conformation, resulting in a smaller interaction between free-radical orbital and C-H bond, hence the higher barrier. The trend found here that *cis*-HONO is favored differs from the trend of the HONO formation in MMH/NO_2 system[14], which has multiple polar N-H bonds allowing *trans*-HONO to interact with both the breaking N-H bond via the O atom and the adjacent N-H bond through the N atom on NO_2, lowering the barrier. The barrier for NO_2 to abstract H on the linker ethyl group is 8.0 kcal/mol, essentially the same as the 8.3 kcal/mol to abstract H from the terminal methyl group. The increased entropy for bringing these two gas phase molecules together at the TS raises the Gibbs free energy by about 10 kcal/mol for both reactions. To separate the product complex of HONO and TMEDA free radical to form intermediates INT1 and INT2 requires another 7~8 kcal/mol. Comparing with TMEDA, the barriers of HONO formation from 2,5-dimethyl-hexane are about 10 kcal/mol higher, indicating that the N atom adjacent to the C-H bond both reduces the C-H bond energy as shown before and also lowers the barrier for HONO abstraction. At the TS, the nitrogen donates its lone pair electrons to the antibonding C-H orbital, stabilizing the TS and lowering the barrier.

Besides the two HONO formation pathways to form INT1 and INT2, we found that simultaneous attack of two NO_2 to both ends of the relative weak C-C bond (TS3, Figure 4-3c), breaks the C-C

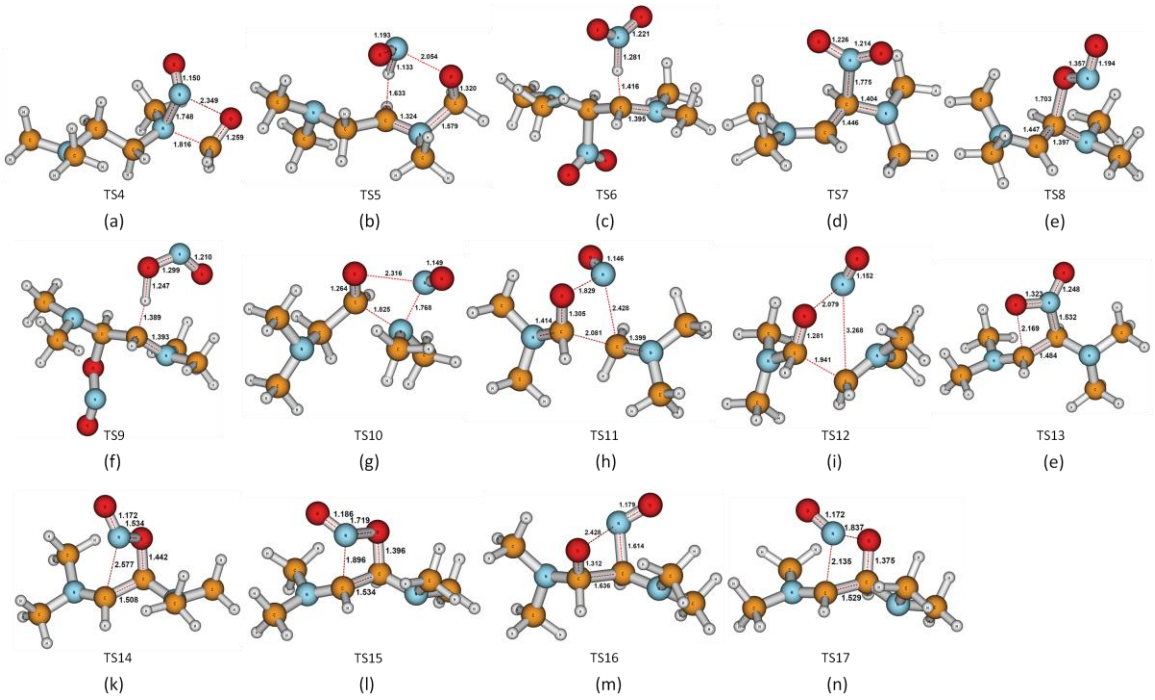

Figure 4-4. Structures of (a)TS4 (b)TS5 (c)TS6 (d)TS7 (e)TS8 (f)TS9 (g)TS10 (h)TS11 (i)TS12 (j)TS13 (k)TS14 (l)TS15 (m)TS16 (n)TS17

bond to form two ONO-$CH_2N(CH_3)_2$ fragments. This path leads to an unusually low enthalpy barrier (10.3 kcal/mol) for C-C bond breaking because that the lone pair electrons of both N atoms donate into the C-C antibonding orbital from both ends. This stabilizes both free radicals formed upon C-C bond dissociation as shown before. However this requires a termolecule-reaction, leading to an entropy decrease that raises the free energy at the TS to 30.0 kcal/mol, making this pathway unlikely in the gas phase. On the other hand, for the condensed mixture of TMEDA and HNO_3, where NO_2 molecule is the solute, this entropy cost will decrease, reducing the free energy barrier to make this pathway more viable.

3.2 Reactions after INT 1

After H-abstraction, the TMEDA free radical on the terminal methyl group, INT1, can recombine with other NO_2 radicals. The recombinations to form INT4 and INT5 are about 46 kcal/mol exothermic with no barriers. From INT4, it is quite favorable to eliminate the NO, leaving an O

radical on the fragment. This O radical can then form a C-O double bond while breaking the C-N bond, leaving a bimolecular-like state, of formaldehyde molecule plus an N radical. The dissociating NO can either recombine with N radical (TS4, Figure 4-4a) to form INT9 with a barrier 29.0 kcal/mol, or abstract one H from C (TS5, Figure 4-4b) to form a C-N double bond and HNO molecule (INT10) but with a much higher barrier, 42.5 kcal/mol. The nitro compound INT5 is less reactive and may play a small role at the initial stage when temperature is low.

3.3 Reactions after INT2

Similar to INT1, the free radical on the middle ethyl of TMEDA, INT2, can recombine with another NO_2 free radical to form nitro and nitrite compounds, INT6 and INT8, without a barrier while releasing more than 45 kcal/mol of energy. INT6 and INT8 can lose H again through HONO formation via TS6 (Figure 4-4c) and TS9 (Figure 4-4f) to form free radical intermediate INT11 and INT12 with barriers about 8kcal/mol, similar to barriers to lose the first H.

In addition to recombination, NO_2 can also abstract H on the carbon next to the radical site to form a C-C double bond (INT7), which is also barrierless and exothermic by 37.9 kcal/mol. These three reactions are very exothermic and non-reversible. Consequently, their relative reaction rates to form INT6, INT7 and INT8 may be dominated by the kinetics of interactions with the NO_2, rather than the thermodynamics of products formation.

The NO_2 can open the double bond in INT7, converting to INT11 via TS7 (Figure 4-4d), and INT12 via TS8 (Figure 4-4e). The TS we located for opening double bond (TS8) to form INT12, has a lower energy than INT12 after including the zero point energy (ZPE),

suggesting that INT12 is not be a stable intermediate in gas phase, but it may play a role in the condensed phase.

The formation of INT7 containing the C-C double bond is important because this double bond is fairly easily to oxidize in acid (compared with the saturated bonds). Some possible low barrier mechanisms for C-C and C-N bond breaking are proposed and discussed below.

Like INT4, INT8 can decompose unimolecularly to eliminate NO from the -ONO group. The subsequent formation of the C-O double bond can lead to:

1. C-N bond breaking and N-N bond formation (via TS10, Figure 4-4g) to form INT13. Indeed the ON-N$(CH_3)_2$ moiety has been identified in the IR spectrum of the gas product of TMEDA and HNO_3[7].
2. C-C bond breaking (via TS11 and TS12, see Figure 4-4h and i). TS11 is 17.2 kcal/mol lower than TS12 due to the less strained geometry, despite the new C-N bond and greater exothermicity of the product from TS12. Although INT14 and INT10 are similar, TS10 is 7.5 kcal/mol lower than TS5 because the formaldehyde C-O double bond is weaker than the primary aldehyde bond in INT14.

Comparing with the above unimolecular reactions (involving favorable entropic effects), the H-abstraction by NO_2 has the lowest enthalpic barrier (8.1) and free energy barrier (17.8 kcal/mol) (TS9, Figure 4-4f). The product free radical can react with the O in the -ONO group to form an epoxide (INT19) and NO via TS17 (Figure 4-4h), or it can react with the N to form a 4-member ring intermediate, INT17, with negligible barrier (< 2 kcal/mol). With the help of lone pairs on N atoms, breaking the C-C bond in the 4-member ring intermediate has a barrier of only 8.1 kcal/mol. This ring breaking reaction starts with N-O bond breaking,

followed by C-O double bond formation, leading to C-C bond fission (TS16, Figure 4-4m) to release 41.9 kcal/mol. In addition to the considerable exothermicity, this reaction produces two reactive fragments, an amino aldehyde and a free radical, that can induce further reactions. The amino aldehyde products is stable and has been observed via IR spectroscopy[7] as a gas product of the reaction between TMEDA and HNO_3. This differs from the free radical recombination, which reduces the number of reactive molecules and is entropically unfavorable.

4. Reaction mechanism of TMMDA+NO_2

The reactions of TMMDA with NO_2 are similar to those between TMEDA and NO_2, except there is no C-C double bond formation and C-C bond breaking. Three types of reactions are:

1. H abstraction by NO_2 (reactions to INT20 and INT21) leaving a free radical on TMMDA.
2. Free radical recombination of NO_2 with the product from H abstraction (reactions to INT22, INT23, INT24 and INT25).
3. Breaking the C-N bond on TMMDA to form a new N-N bond (reactions to INT26 and INT28) or a C-N double bond (reaction to INT27).

The enthalpy and Gibbs free energy of each species is marked in Figure 4-5 and referenced to the sum of individual TMMDA and NO_2 energies in the gas phase.

4.1. Initiating stage: H-abstraction.

The reaction starts with NO_2 abstracting H on the terminal methyl groups (via TS18, Figure 4-6a, to INT20) or the middle $–CH_2-$ group (via TS19, see Figure 4-6b to INT21) to form HONO. All barriers are very similar to those of TMEDA. Although the lone-pair electron on nitrogen can stabilize the TS for H-abstraction, as seen for TMEDA, abstracting the H from the middle methyl group between two nitrogen atoms does not get a double effect because the lone-pairs on neighboring nitrogen atoms orient perpendicular to each other due to steric repulsion so that only one lone-pair has the right orientation to donate electron into the antibonding orbital of C-H bond to stabilize the transition state. As a result, the barrier height of 8.8kcal/mol is similar to same reactions in TMEDA.

4.2. Reactions after INT20

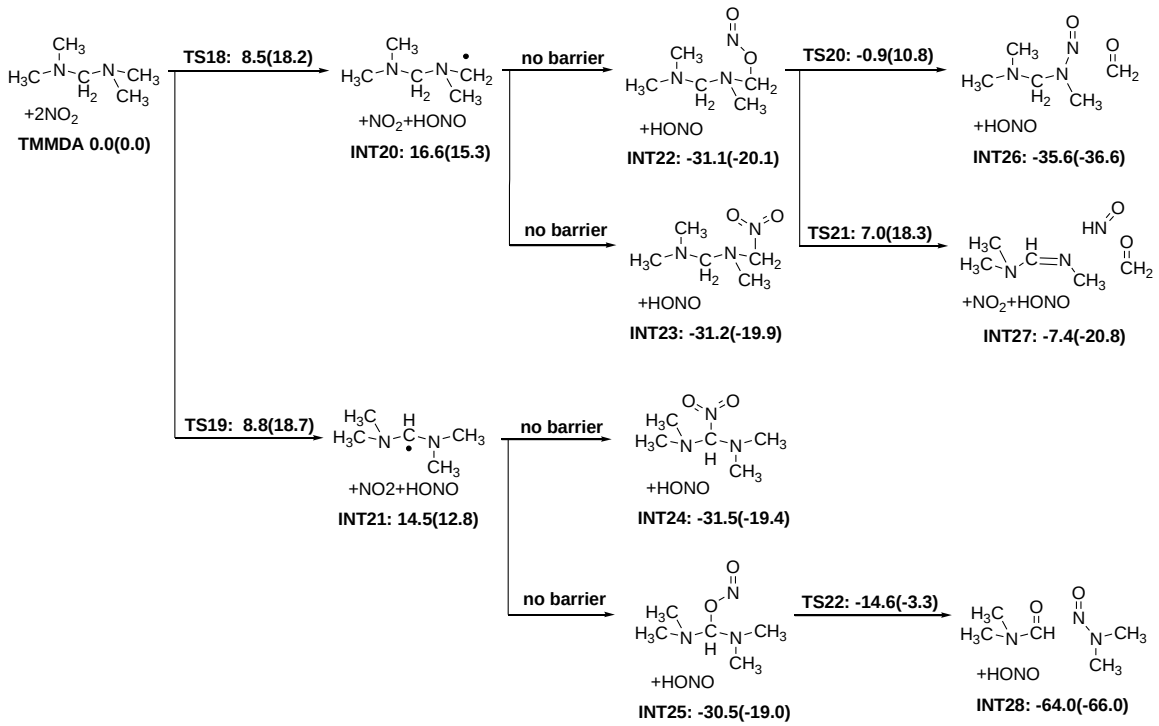

Figure 4-5 Reactions between TMMDA and NO_2. Enthalpy and Gibbs free energy (in parentheses) of each species are provided in kcal/mol.

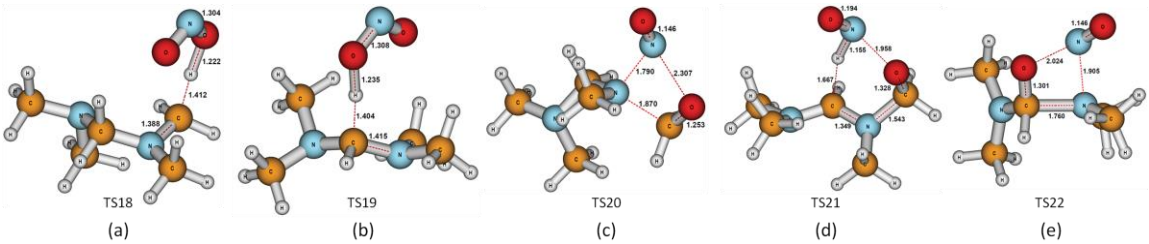

Figure 4-6. Structures of (a)TS18 (b)TS19 (c)TS20 (d)TS21 (e)TS22

Without the possibility of forming a C-C double bond, the only favorable pathway to oxidize TMMDA is via free radical recombination to generate nitro or nitrite compounds (INT22, INT23, INT24 and INT25). All reactions are exothermic by 30 to 31 kcal/mol. The nitrite compound can undergo unimolecular reaction to break the C-N bond while forming the C-O double bond to generate formaldehyde, followed by forming a N-N bond (via TS20, Figure 4-6c, to INT26) or a C-N double bond (via TS21, Figure 4-6d, INT27), which are similar to reactions to INT9 and INT10 in Figure 4-2.

The same C-N bond breaking and C-O double bond formation can also take place on INT25 via TS22 (Figure 4-6e), generating an amino aldehyde and a N-nitroso fragment with a 15.9 kcal/mol barrier, releasing considerable energy, 33.5 kcal/mol. This path also generates two reactive fragments that can each be further oxidized easily.

5. Comparison between reaction mechanisms of TMEDA/NTO and TMMDA/NTO

In both systems, the initiation reaction is HONO formation, which is also observed experimentally in hydrazine derivative/NTO[12, 15] and NH_3/NTO[16] systems. This step has a low barrier but is endothermic, making it not helpful for initiating other reactions that might have higher barriers. The exothermic steps usually involve the oxidation of C, such as free radical recombination (forming a new C-N or C-O bond) or C-O double bond formation. The barrier to oxidize carbon via a free radical recombination pathway is similar for both TMEDA and TMMDA, since these

free radicals are generated by HONO formation, which has barrier around 8-9 kcal/mol for both fuels. However, C oxidation via C-O double bond formation has quite different barriers for TMEDA and TMMDA. In TMMDA, the most favorable pathway to form the C-O double bond is from INT25 to INT28, which has a barrier 15.9 kcal/mol. In contrast, for TMEDA, this can occur via several pathways. Starting from intermediate INT7 with a C-C double bond, the highest barrier on the pathway to reach the product with a C-O double bond, INT18, is 8.1 kcal/mol (at TS16). This lower barrier for C oxidation leads to faster heat releasing, which may account for the shorter ignition delay observed experimentally.

Based on the above comparisons, the higher reactivity of TMEDA towards NO_2 is due to the formation and oxidation of the C-C double bond on the ethyl linker. The C-H bond adjacent to N atom is easier to break due to the lone pair stabilization, and TMEDA has two such C-H bonds on the ethyl linker, favoring formation of a double bond intermediate that can undergo further oxidization. The double bond can also be opened and oxidized by nitric acid.

In contrast, although TMMDA has five carbon atoms adjacent to N atoms, they are not connected to each other, so that formation of a C-C double bond is impossible for TMMDA. The same mechanism can also be applied to explain the reactivity difference between DMPipZ and TMTZ, where DMPipZ has two adjacent carbons leading to short ignition delay, while TMTZ has no pairs of adjacent carbons and is non-hypergolic.

6. Comparison between the initiation of diamines (TMEDA and TMMDA) and their dinitrate salts (TMEDADN and TMMDADN)

To illustrate how salt formation affects the reactivity of these fuels, we calculated the H-abstraction by NO_2 from the TMEDA (TMMDA)-dinitric acid complex in gas phase, as shown in

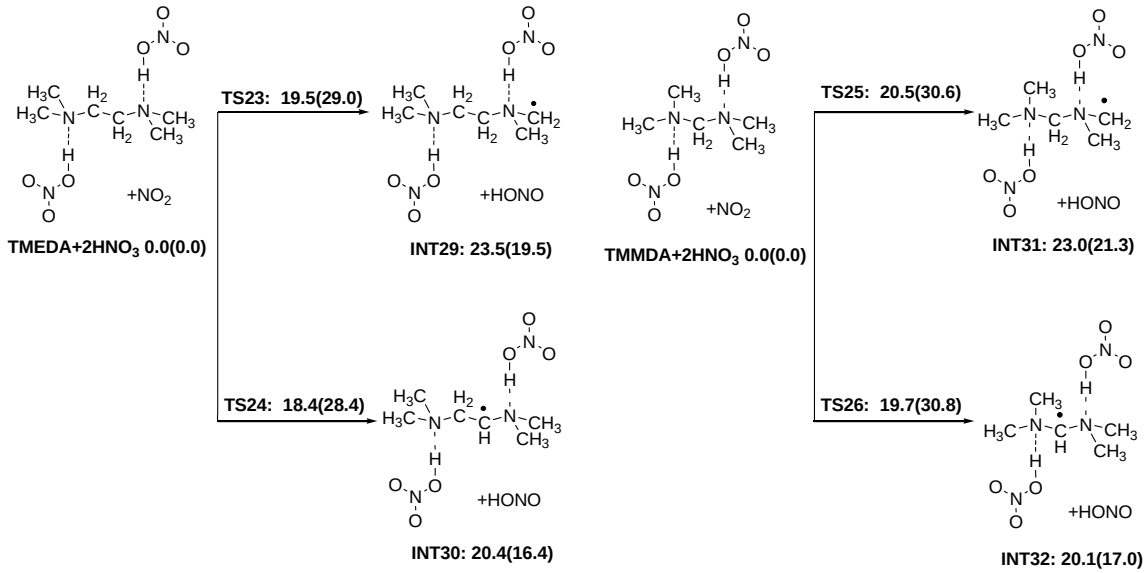

Figure 4-7. Initiation reactions between TMEDA(TMMDA)-2HNO_3 complex and NO_2. The enthalpy and Gibbs free energy (in parentheses) of each species are provided in kcal/mol.

Figure 4-7. Without solvent stabilization, proton transfer and salt formation are not favored in vacuum, as indicated by the longer N-H distance (1.580Å in TMEDA-2HNO_3 and 1.665Å in TMMDA-2HNO_3) and shorter O-H distance (1.049Å in TMEDA-2HNO_3 and 1.030Å in TMMDA-2HNO_3). However, although the proton transfer and salt formation are not as complete for gas phase as for the polar solvent, we still observe considerable chemical differences between amine and the amine-HNO_3 complex, which provides insight about the reactivity of TMEDADN and TMMDADN with fully transferred protons.

TS geometries of H-abstraction on two amine-HNO_3 complexes are shown in Figure 4-8. The barriers for these reactions are ~10 kcal/mol higher than those for the pure amines. The final amine-HNO_3 radicals (INT29-32) are also ~8 kcal/mol less stable than the pure amine-radicals (INT1, INT2, INT 20 and INT21), which can be explained as follows. As indicated in Section 2 and 3, lone pairs on N play an important role on lowering the barriers of H-abstraction by donating electron density into the antibonding orbital of adjacent C-H bonds. In amine-HNO_3 complexes, the electron density of lone pair of N is drawn to the proton on the nitric acid and less

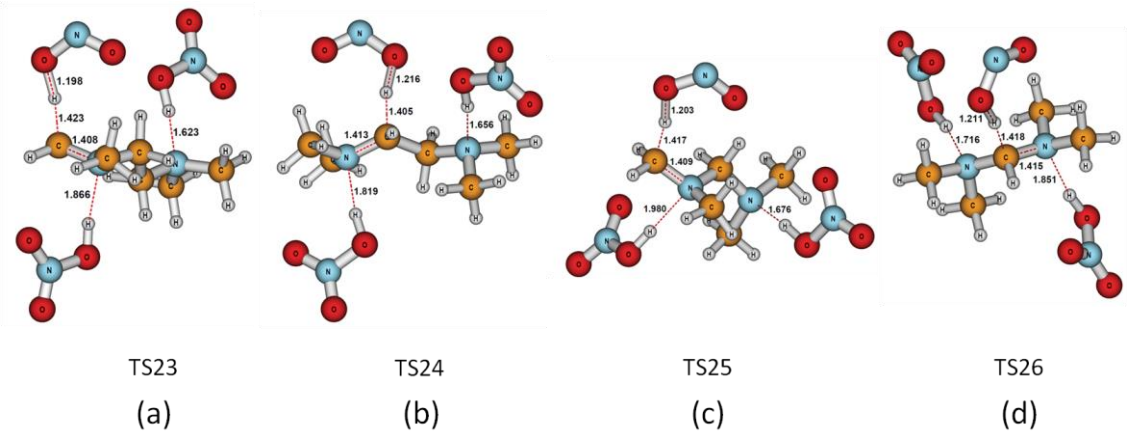

Figure 4-8. Structures of (a)TS23 (b)TS24 (c)TS25 (d)TS26

capable of donating into the C-H antibonding orbital, resulting in higher barriers and less stable final products. At TS23-25, the N-H distances on the side at which H-abstraction is taking place are ~0.2Å longer than the N-H bond distances on the other side, indicating that the C-H antibonding orbital is competing with the N-H bond for the electron density of lone pair on N, pushing the proton away from N and leading to the extra energy cost for reaction to proceed. It is reasonable to conclude that when protons are fully transferred, the lone pair on N is more confined and localized in the N-H bond region and not able to interact with nearby vacant orbital or free radicals, resulting in even higher barrier and endothermicity of H-abstraction. In other words, the salt formation uses the long pair electrons on N to form N-H bonds while the product salt is similar to the corresponding alkane, which is chemically inert. This leads to the dinitrate salt playing a less important role in the early stage of ignition.

Conclusion

DFT calculations of energetics for various reactions involved in the hypergolic reaction of HNO_3 with TMEDA and TMMDA lead to an atomistic chemical mechanism that explains the dramatic

difference in pre-ignition delay between these two fuels. We find two key factors and illustrate how the molecular structure relates to the ignition delay.

- The first factor is the exothermicity of the formation of the dinitrate salt of TMEDA and TMMDA. Due to the shorter distance between basic amines in TMMDA, it is more difficult to protonate both amines for the stronger electrostatic repulsion, resulting in the heat of dinitrate salt formation being smaller by 6.3 kcal/mol.
- The second factor is the reaction rate of TMEDA and TMMDA reacting with NO_2 to the step that releases sufficient heat and additional reactive species to propagate reaction. In TMEDA, the formation of the intermediate with C-C double bond and the low bond energy of C-C single bond provide a route with low barrier to oxidize C.

Both factors can contribute to the shorter ignition delay of TMEDA. The same reasoning based on the molecular structure can be applied to other fuels, such as DMPipZ and TMTZ. These results indicate that TMEDA and DMPipZ are excellent green replacements for hydrazines as the fuel in bipropellants.

References

1. Catoire, L.; Chaumeix, N.; Pichon, S.; Paillard, C., *J. Propul. Power* **2006,** *22* (1), 120-126.
2. Osmont, A.; Catoire, L.; Klapotke, T. M.; Vaghjiani, G. L.; Swihart, M. T., *Propellants Explosives Pyrotechnics* **2008,** *33* (3), 209-212.
3. Pichon, S.; Catoire, L.; Chaumeix, N.; Paillard, C., *J. Propul. Power* **2005,** *21* (6), 1057-1061.
4. Nonnenberg, C.; Frank, I.; Klapotke, T. M., *Angew. Chem., Int. Ed.* **2004,** *43* (35), 4585-4589.

5. Frota, O. M., B.; Ford, M., *Proceedings of the 2nd International Conference on Green Propellants for Space Propulsion (ESA SP-557).* **2004**.

6. Co., P. P., Petroleum Derivable Nitrogen Compounds as Liquid Rocket Fuels. In *Report 1478-56R, Phillips Petroleum Co*, 1956.

7. Wang, S. Q.; Thynell, S. T.; Chowdhury, A., *Energy Fuels* **2010,** *24*, 5320-5330.

8. Wang, S. Q.; Thynell, S. T., *unpublished result. The experimental setting to measure the ignition delay is the same as described in Ref 4* **2010**.

9. McQuaid, M. J.; Stevenson, W. H.; Thompson, D. M., *Proceedings for the Army Science Conference (24th)* **2005**.

10. Chen, C.-C.; Nusca, M. J.; McQuaid, M. J. *Modeling Combustion Chamber Dynamics of Impinging Stream Vortex Engines Fueled with Hydrazine-Alternative Hypergols*; 2008.

11. Addison, C. C., *Chem. Rev. (Washington, DC, U. S.)* **1980,** *80* (1), 21-39.

12. Stone, D. A., *Toxicol. Lett.* **1989,** *49* (2-3), 349-360.

13. Klapotke, T. M.; Harcourt, R. D.; Li, J. B., *Inorg. Chim. Acta* **2005,** *358* (14), 4131-4136.

14. McQuaid, M. J.; Ishikawa, Y., *J. Phys. Chem. A* **2006,** *110* (18), 6129-6138.

15. Catoire, L.; Chaumeix, N.; Paillard, C., *J. Propul. Power* **2004,** *20* (1), 87-92.

16. Bedford, G.; Thomas, J. H., *Journal of the Chemical Society-Faraday Transactions I* **1972,** *68* (11), 2163-2170.